Contribution from the Laboratory for Molecular Structure and Bonding, Department of Chemistry, Texas A&M University, College Station, Texas 77843

Luminescent Extended One-Dimensional Heterobimetallic Chain Compounds with Relativistic Metal–Metal Bonds. Synthesis, Crystal Structures, and Spectroscopic Studies of $AuTl(MTP)_2$ and $Au_2Pb(MTP)_4$ (MTP = $[CH_2P(S)Ph_2]^-$)

Suning Wang, Guillermo Garzón, Christopher King, Ju-Chun Wang, and John P. Fackler, Jr.*

Received July 25, 1989

The heterobimetallic complexes $AuTl(CH_2P(S)Ph_2)_2$ (**2**) and $Au_2Pb(CH_2P(S)Ph_2)_4$ (**3**) were obtained in good yields from the reactions of $PPN[Au(CH_2P(S)Ph_2)_2]$ (**1**) with Tl_2SO_4 and $Pb(NO_3)_2$, respectively. Their structures were determined by single-crystal X-ray diffraction. Compounds **2** and **3** form extended one-dimensional linear chain polymers with short metal–metal separations (~3.0 Å) in the solid state. **2** crystallizes in the $P2_1/a$ space group with unit cell dimensions a = 24.368 (4) Å, b = 11.655 (2) Å, c = 9.445 (2) Å, β = 101.13 (2)°, V = 2632.2 (8) Å^3, and Z = 4, while **3** crystallizes in the $I2/a$ ($C2/c$) space group with unit cell dimensions a = 22.476 (5) Å, b = 9.008 (2) Å, c = 31.476 (8) Å, β = 107.19 (2), V = 6088 (2) Å^3, and Z = 4. Both of **2** and **3** are strongly luminescent when irradiated with UV light. The solid of **2** emits at 575 nm (298 K) with a lifetime of 0.98 μs, while the solid of **3** emits at 752 nm (298 K) with a lifetime of 22 ns. Luminescence is attributed to interactions between metal atoms in these compounds. Studies of the solid of **3** by scanning electron microscopy (SEM) indicate that fibers of **3** are either conducting or semiconducting.

Introduction

Extended linear chain compounds have attracted the attention of chemists and physicists for many years because of their fascinating and unique chemical and physical properties.[1,2] Although numerous extended chain compounds have been reported, the syntheses of these compounds and the rationalization of the bonding of one-dimensional chain structures still remain as a challenge to chemists and theorists. Among the known one-dimensional chain compounds, few are bimetallic. Some gold(I) dimers with sulfur-coordinated chelating ligands have been known to form one-dimensional chains in the solid state with various Au(I)···Au(I) separations (2.76–3.40 Å).[3] However, heterobimetallic analogues were previously unknown. The synthesis and characterization of heterobimetallic linear chain compounds, II, have thus become of special interest to us. Upon reaction of $PPN[Au(MTP)_2]$ (PPN = $[(Ph_3P)_2N]^+$; MTP = $[CH_2P(S)Ph_2]^-$) with appropriate metal ions, $Au_2Pt(MTP)_4$, $Au_2Pb(MTP)_4$, and $AuTl(MTP)_2$ have been prepared. Each is a one-dimensional chain in the solid state. The structure of $Au_2Pt(MTP)_4$ was reported earlier.[4] The structure of $AuTl(MTP)_2$ has been described in an preliminary communication.[5]

The compounds $Au_2Pb(MTP)_4$ and $AuTl(MTP)_2$ not only have unique one-dimensional structures but also show very interesting properties of luminescence. Although a variety of luminescent organometallic complexes have been reported,[6] most are metal carbonyl complexes or binuclear or polynuclear transition-metal complexes with at least one metal atom in a d^8 electronic configuration.[6,7] Very little is known about luminescent binuclear or polynuclear metal complexes with d^{10} and s^2 electronic configurations. Recently Gray et al. have described the luminescence of binuclear palladium and platinum complexes with d^{10}–d^{10} configuration.[8a] We have also discovered that a number of gold(I) dimers are luminescent.[8b] We report here the syntheses and characterization of $AuTl(MTP)_2$ and $Au_2Pb(MTP)_4$ and the spectroscopic study of their fascinating luminescence, the first extended linear chain heterobinuclear and heterotrinuclear species showing such behavior.[8c]

Results and Discussion

Synthesis and Characterization of $AuTl(MTP)_2$ (2) and $Au_2Pb(MTP)_4$ (3). The reagent $PPN[Au(MTP)_2]$ (**1**) has been found to be very useful for the synthesis of heterobimetallic complexes. **1** reacts readily with M^+ or M^{2+} cations to generate the corresponding neutral bimetallic species. The yellow crystalline compound $AuTl(MTP)_2$ (**2**) was obtained in 64% yield by the addition of a methanol solution of Tl_2SO_4 to the CH_2Cl_2 solution of **1** in a 1:1 ratio of Au:Tl. Addition of a solution of $Pb(NO_3)_2$ in methanol to a CH_2Cl_2 solution of **1** in a 1:2 ratio resulted in the formation of the bronze-colored crystalline $Au_2Pb(MTP)_4$ (**3**) in 72% yield.

The ^1H spectra show the methylene doublet of the MTP ligand in **2** and **3** is shifted downfield (δ = 1.64 ppm, J_{P-H} = 12 Hz, in $CDCl_3$, for **2**; δ = 1.71 ppm, J_{P-H} = 12 Hz, in $CDCl_3$, for **3**) from that of **1** (δ = 1.52 ppm, J_{P-H} = 15 Hz, in $CDCl_3$). These shifts are independent of concentration, indicating the presence of a bonding interaction of the Tl(I) ion or Pb(II) ion with the Au-$(MTP)_2^-$ anion. The ^1H NMR spectra of **2** and **3** show no coupling of $-CH_2$ groups with Tl (^{205}Tl, $I = {}^1/_2$, natural abundance 70%) or Pb (^{207}Pb, $I = {}^1/_2$, natural abundance 23%), an indication that the bonding of the Tl^+ ion or Pb^{2+} ion with the $Au(MTP)_2^-$ anion is through the sulfur atoms of $Au(MTP)_2^-$. The presence of bonding interactions of Pb^{2+} with $Au(MTP)_2^-$ in solution is also supported by the ^{31}P NMR spectrum of $Au_2Pb(MTP)_4$, showing a singlet at 50.5 ppm with two ^{31}P–^{207}Pb coupling satellites, J_{P-Pb} = 16 Hz. A similar coupling was not observed for $AuTl(MTP)_2$, probably due to the small coupling constant of ^{31}P with ^{205}Tl.

Both compounds **2** and **3** were studied by scanning electron microscopy (SEM). Without a conductive coating, crystals of **2** did not yield a clear image due to the charging effects. In contrast, the bronze-colored (solvent free) crystals of **3** gave a very sharp SEM image, indicating that the compound **3** is conducting or semiconducting.[9] SEM photographs show that the solid of **3** has a one-dimensional fiberlike morphology (Figure 1). The powder reflectance spectrum of **3** (Figure 2) shows a broad band in the visible region with a cutoff at ca. 600 nm, suggesting the

* To whom correspondence should be addressed.

(1) Miller, J. S., Ed. *Extended Linear Chain Compounds*; Plenum: New York and London, 1981–1983; Vol. 1–3.
(2) Hoffmann, R. *Angew. Chem., Int. Ed. Engl.* **1987**, *26*, 846.
(3) (a) Mazany, A. A.; Fackler, J. P., Jr. *J. Am. Chem. Soc.* **1984**, *106*, 801. (b) Mazany, A. A. Ph.D. Thesis, Case Western Reserve University, 1984. (c) Jones, P. G. *Gold Bull.* **1981**, *14*, 102.
(4) Murray, H. H.; Briggs, D. A.; Garzon, G.; Raptis, R. G.; Porter, L. C.; Fackler, J. P., Jr. *Organometallics* **1987**, *6*, 1992.
(5) Wang, S.; Fackler, J. P., Jr.; King, C.; Wang, J. C. *J. Am. Chem. Soc.* **1988**, *110*, 3308–3310.
(6) (a) Lees, A. J. *Chem. Rev.* **1987**, *87*, 711. (b) Ferraudi, G. J. *Elements of Inorganic Photochemistry*; John wiley & *Sons*: New York, 1988.
(7) (a) King, C.; Auerbach, R. A.; Fronczek, F. R.; Roundhill, D. M. *J. Am. Chem. Soc.* **1986**, *108*, 5626. (b) Fordyce, W. A.; Brummer, J. G.; Crosby, G. A. *J. Am. Chem. Soc.* **1981**, *103*, 7061. (c) Mann, K. R.; Lewis, N. S.; Williams, R. M.; Gray, H. B.; Gordon, J. C., II. *Inorg. Chem.* **1978**, *17*, 828. (d) Balch, A. L.; Nagle, J. K.; Olmstead, M. M.; Reedy, P. E., Jr. *J. Am. Chem. Soc.* **1987**, *109*, 4123.
(8) (a) Harvey, P. D.; Gray, H. B. *J. Am. Chem. Soc.* **1988**, *110*, 2145. (b) King, C.; Wang, J. C.; Khan, Md. N. I.; Fackler, J. P. Jr. *Inorg. Chem.* **1989**, *28*, 2145–2149. (c) See also: Balch, A. L.; Davies, B. J.; Olmstead, M. M. *Inorg. Chem.* **1989**, *28*, 3148.
(9) Goldstein, J. I., et al., Eds. *Scanning Electron Microscopy and X-Ray Microanalysis*; Plenum Press: New York and London, 1981.

0020-1669/89/1328-4623$01.50/0

Figure 1. Scanning electron micrograph of $Au_2Pb(MTP)_4$ not coated with conducting film.

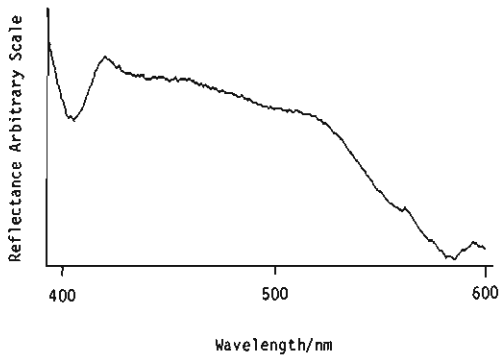

Figure 2. Powder reflectance spectrum of **3**.

Table I. Crystallographic Data for $AuTl(MTP)_2$ (**2**) and $Au_2Pb(MTP)_4$ (**3**)

formula	$C_{26}H_{24}TlAuS_2P_2$	$C_{52}H_{48}PbAu_2S_4P_4 \cdot 2C_4H_8O$
fw	863.4	1670.5
space group	$P2_1/a$	$I2/a$
a, Å	24.368 (4)	22.476 (6)
b, Å	11.655 (2)	9.008 (2)
c, Å	9.445 (2)	31.476 (8)
β, deg	101.13 (2)	107.19 (2)
V, Å^3	2632.2 (8)	6088 (2)
Z	4	4
d_{calc}, g cm^{-3}	2.18	1.82
cryst size, mm	0.10 × 0.20 × 0.20	0.30 × 0.40 × 0.80
$F(000)$, e	1608	3216
μ(Mo Kα), cm^{-1}	120.2	78.2
radiation (Mo Kα), Å	0.71069	0.71069
temp, °C	22	22
scan method	ω	ω
2θ range, deg	2–45	2–45
no. of reflcns measd	3950	4443
no. of reflcns for $F_o^2 \geq 3\sigma(F_o^2)$	1659	1524
no. of params refined	111	137
transm factor: max, min	1.00, 0.44	0.79, 0.72
R^a	0.0625	0.0351
R_w^b	0.0647	0.0405
goodness-of-fit indicator^c	1.341	1.356
largest shift/esd (final cycle)	0.003	0.004
largest peak, e/Å^3	3.44	0.78

$^a R = \sum||F_o| - |F_c||/\sum|F_o|$. $^b R_w = [\sum w^{1/2}(|F_o| - |F_c|)]/\sum w^{1/2}|F_o|$; $w^{-1} = [\sigma^2(|F_o|) + |g|F_o^2]$; $g = 0.001\,46$ for **2**, $g = 0.000\,30$ for **3**. ^{c}Goodness-of-fit $= [\sum w(|F_o| - |F_c|)^2/(N_o - N_p)]^{1/2}$.

presence of nondiscrete levels in the ground and/or excited state(s).

Both **2** and **3** glow with a distinctive colored luminescence in the solid state when irradiated by a UV lamp. **2** strongly emits a yellow-orange color, while **3** emits a red color in the solid state and a yellow color in solution. In order to understand these unusual phenomena, single-crystal X-ray diffraction structural analysis and excitation and emission spectroscopic studies were performed. Theoretical calculations using the Fenske–Hall method were carried out for both compounds.

Table II. Atomic Coordinates (×10^4) and Isotropic Thermal Parameters (Å^2 × 10^3) for **2**^{a}

atom	x	y	z	U_{iso}^{b}
Au	2450 (1)	2980 (1)	5425 (2)	39 (1)*
Tl	2369 (1)	449 (1)	5273 (2)	58 (1)*
P(1)	3706 (4)	2357 (7)	5256 (10)	38 (3)*
P(2)	1439 (4)	2445 (8)	2650 (12)	53 (4)*
S(1)	3425 (4)	1008 (9)	4111 (13)	67 (5)*
S(2)	1680 (6)	882 (10)	2442 (15)	93 (6)*
C(1)	3299 (10)	2781 (22)	6627 (28)	16 (6)
C(2)	1588 (10)	3163 (22)	4480 (28)	19 (6)
C(11)	4115 (8)	4486 (19)	4623 (21)	51 (9)
C(12)	4126 (8)	5464 (19)	3777 (21)	65 (11)
C(13)	3782 (8)	5532 (19)	2416 (21)	68 (11)
C(14)	3427 (8)	4623 (19)	1901 (21)	57 (10)
C(15)	3416 (8)	3645 (19)	2747 (21)	62 (11)
C(16)	3760 (8)	3577 (19)	4108 (21)	35 (8)
C(21)	4617 (10)	2460 (22)	7560 (27)	82 (13)
C(22)	5171 (10)	2242 (22)	8215 (27)	115 (18)
C(23)	5524 (10)	1669 (22)	7453 (27)	87 (14)
C(24)	5324 (10)	1314 (22)	6037 (27)	86 (14)
C(25)	4770 (10)	1532 (22)	5383 (27)	82 (13)
C(26)	4417 (10)	2105 (22)	6144 (27)	46 (9)
C(31)	1937 (11)	2867 (16)	312 (29)	74 (12)
C(32)	2123 (11)	3566 (16)	−699 (29)	91 (15)
C(33)	2069 (11)	4755 (16)	−626 (29)	84 (13)
C(34)	1830 (11)	5245 (16)	459 (29)	107 (16)
C(35)	1644 (11)	4546 (16)	1469 (29)	81 (13)
C(36)	1698 (11)	3357 (16)	1396 (29)	57 (10)
C(41)	389 (13)	1495 (22)	1800 (33)	98 (16)
C(42)	−193 (13)	1502 (22)	1403 (33)	142 (22)
C(43)	−484 (13)	2539 (22)	1303 (33)	110 (17)
C(44)	−193 (13)	3569 (22)	1600 (33)	104 (17)
C(45)	389 (13)	3562 (22)	1997 (33)	89 (15)
C(46)	680 (13)	2525 (22)	2097 (33)	69 (12)

^{a}Estimated standard deviations in the least significant digits are given in parentheses. ^{b}For values with asterisks, the equivalent isotropic U is defined as one-third of the trace of the U_{ij} tensor.

Table III. Bond Lengths (Å) and Angles (deg) for **2**^{a}

Au–Tl	2.959 (2)	Au–C(1)	2.170 (22)
Au–C(2)	2.128 (23)	Au–Tl′	3.003 (2)
Tl–S(1)	3.055 (12)	Tl–S(2)	2.914 (13)
P(1)–C(1)	1.845 (29)	P(1)–S(1)	1.957 (14)
P(1)–C(26)	1.796 (24)	P(1)–C(16)	1.808 (23)
P(2)–C(2)	1.892 (28)	P(2)–S(2)	1.935 (16)
P(2)–C(46)	1.824 (32)	P(2)–C(36)	1.795 (28)
Tl–Au–C(1)	88.1 (7)	Tl–Au–C(2)	91.6 (7)
C(1)–Au–C(2)	173.4 (10)	Tl–Au–Tl′	162.9 (1)
C(1)–Au–Tl′	93.0 (7)	C(2)–Au–Tl′	89.2 (7)
Au–Tl–S(1)	75.6 (2)	Au–Tl–S(2)	83.9 (2)
S(1)–Tl–S(2)	90.5 (4)	Au–Tl–Au′	162.7 (1)
S(1)–Tl–Au′	87.5 (2)	S(2)–Tl–Au′	92.7 (2)
S(1)–P(1)–C(1)	115.1 (9)	S(1)–P(1)–C(16)	111.0 (8)
C(1)–P(1)–C(16)	108.8 (11)	S(1)–P(1)–C(26)	109.3 (10)
C(1)–P(1)–C(26)	108.4 (12)	C(16)–P(1)–C(26)	103.5 (11)
S(2)–P(2)–C(2)	120.0 (10)	S(2)–P(2)–C(36)	109.7 (10)
C(2)–P(2)–C(36)	108.1 (12)	S(2)–P(2)–C(46)	109.3 (10)
C(2)–P(2)–C(46)	104.2 (13)	C(36)–P(2)–C(46)	104.3 (13)
Tl–S(1)–P(1)	101.7 (5)	Tl–S(2)–P(2)	101.7 (6)
Au–C(1)–P(1)	104.4 (12)	Au–C(2)–P(2)	109.9 (13)
P(1)–C(16)–C(11)	120.0 (6)	P(1)–C(16)–C(15)	119.8 (6)
P(1)–C(26)–C(21)	121.8 (9)	P(1)–C(26)–C(25)	118.2 (9)
P(2)–C(36)–C(31)	119.5 (8)	P(2)–C(36)–C(35)	120.5 (8)
P(2)–C(46)–C(41)	117.4 (8)	P(2)–C(46)–C(45)	122.5 (9)

^{a}Estimated standard deviations in the least significant digits are given in parentheses.

Structures of $AuTl(MTP)_2$ (2) and $Au_2Pb(MTP)_4$ (3). The positional and thermal parameters of **2** are given in Table II. Selected bond distances and angles are listed in Table III. A diagram of the molecular structure of **2** is shown in Figure 3.

The Au(I) center in **2** is linearly coordinated to two carbon atoms, while the Tl(I) center is bonded to two sulfur atoms with the distances of Tl–S(1) = 3.05 (1) Å and Tl–S(2) = 2.91 (1) Å. Similar Tl–S bond distances have been observed in other

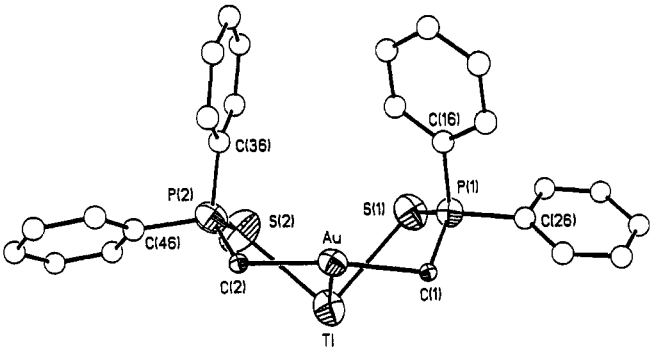

Figure 3. Molecular structure of $AuTl(MTP)_2$ (**2**) showing 50% thermal ellipsoids with the labeling scheme of the atom positions.

Table IV. Atomic Coordinates ($\times 10^4$) and Isotropic Thermal Parameters ($Å^2 \times 10^3$) for **3**[a]

atom	x	y	z	U_{iso}[b]
Au(1)	2500	-428 (1)	0	35 (1)*
Au(2)	2500	6077 (1)	0	40 (1)*
Pb	2500	2787 (1)	0	36 (1)*
P(1)	2031 (3)	5192 (6)	873 (2)	39 (2)*
P(2)	3785 (3)	351 (5)	782 (2)	39 (2)*
S(1)	3825 (3)	2337 (6)	502 (2)	49 (2)*
S(2)	2049 (3)	3000 (5)	797 (2)	48 (2)*
C(1)	1859 (11)	6255 (22)	375 (7)	61 (6)
C(2)	3015 (10)	-432 (19)	687 (6)	45 (5)
C(11)	946 (7)	6475 (15)	969 (4)	67 (7)
C(12)	526 (7)	6808 (15)	1205 (4)	74 (7)
C(13)	628 (7)	6271 (15)	1636 (4)	85 (8)
C(14)	1151 (7)	5401 (15)	1832 (4)	94 (9)
C(15)	1571 (7)	5067 (15)	1596 (4)	78 (7)
C(16)	1468 (7)	5604 (15)	1165 (4)	51 (6)
C(21)	3319 (7)	5084 (13)	1268 (4)	67 (6)
C(22)	3880 (7)	5565 (13)	1562 (4)	110 (10)
C(23)	3889 (7)	6798 (13)	1832 (4)	86 (8)
C(24)	3338 (7)	7550 (13)	1808 (4)	72 (7)
C(25)	2777 (7)	7069 (13)	1514 (4)	57 (6)
C(26)	2767 (7)	5836 (13)	1243 (4)	43 (5)
C(31)	4823 (7)	-480 (13)	529 (5)	79 (8)
C(32)	5242 (7)	-1505 (13)	448 (5)	87 (8)
C(33)	5133 (7)	-3023 (13)	471 (5)	100 (9)
C(34)	4603 (7)	-3516 (13)	573 (5)	79 (8)
C(35)	4183 (7)	-2492 (13)	654 (5)	72 (8)
C(36)	4293 (7)	-974 (13)	631 (5)	42 (5)
C(41)	3770 (5)	1405 (14)	1607 (4)	56 (6)
C(42)	4002 (5)	1608 (14)	2066 (4)	84 (8)
C(43)	4567 (5)	961 (14)	2302 (4)	74 (7)
C(44)	4899 (5)	110 (14)	2080 (4)	79 (7)
C(45)	4667 (5)	-93 (14)	1621 (4)	64 (6)
C(46)	4102 (5)	554 (14)	1385 (4)	41 (5)
O	1367 (20)	981 (40)	1713 (14)	260 (17)
C(3)	1996 (26)	351 (53)	1745 (17)	207 (20)
C(4)	1870 (34)	-638 (61)	2194 (20)	119 (24)
C(4a)	2359 (27)	-71 (65)	2202 (16)	81 (17)
C(5)	1814 (28)	274 (72)	2435 (18)	90 (22)
C(5a)	2187 (46)	1108 (91)	2384 (28)	147 (36)
C(6)	1472 (17)	1507 (37)	2167 (12)	124 (12)

[a] Estimated standard deviations in the least significant digits are given in parentheses. [b] For values with asterisks, the equivalent isotropic U is defined as one-third of the trace of the U_{ij} tensor.

thallium(I) complexes,[10] such as the thallium(I) dithiocarbamate compounds $[TlS_2CNR_2]$ (R = CH_3, i-C_3H_7, n-C_3H_7). These Tl–S distances are much longer than the sum of nonpolar covalent radii of Tl and S, 2.50 Å, but close to the sum of metallic radii of Tl and S, 2.98 Å.[11,17] Therefore, the Tl–S bonds in **2** are apparently rather weak and largely ionic. This compound forms a one-dimensional chain along the unique crystallographic b axis with nearly equal Tl–Au spacings, as shown in Figure 4. The Tl–Au–Tl′ and Au–Tl–Au′ angles are nonlinear by 17°. The Tl–Au separations in this compound are shorter than the sum of the Tl–Au metallic radii, 3.034 Å,[11,17] suggesting a bonding interaction between the two metal centers. The unsupported intermolecular Tl–Au distance, 3.003 Å, is much shorter than the Au–Pt distance in $Tl_2Pt(CN)_4$ (Tl–Pt = 3.140 Å).[12] Short thallium–transition-metal bonds also have been observed in the complexes $[Ir_2Tl(CO)_2Cl_2\{\mu\text{-}(Ph_2PCH_2)_2AsPh\}_2]NO_3$[13] and $[\{Ru_6C(CO)_{16}\}_2Tl]^+$.[14] Weak Tl···Au interactions with long 3.45-Å separations have been found in $Tl[Au(CN)_2]$.[15] Compound **2**

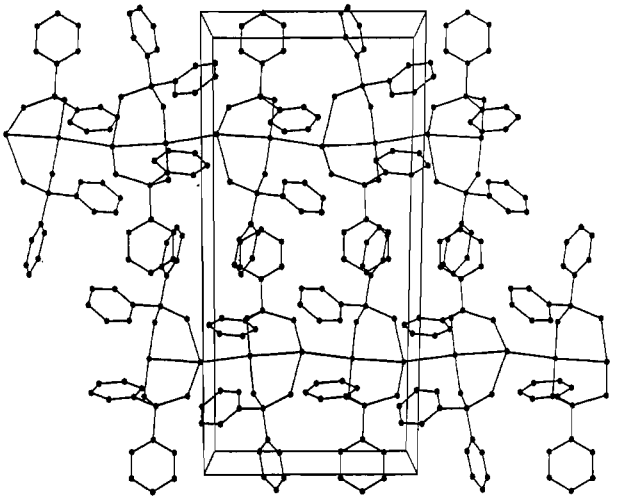

Figure 4. Repeat structure of $AuTl(MTP)_2$ (**2**) in the lattice.

Table V. Bond Lengths (Å) and Angles (deg) for **3**[a]

Au(1)-Pb	2.896 (1)	Au(1)-C(2)	2.129 (17)
Au(2)-Pb	2.963 (2)	Au(2)-C(1)	2.123 (27)
Pb-S(1)	2.959 (5)	Pb-S(2)	2.976 (6)
Au(2)-Au(1)′	3.148 (2)		
P(1)-S(2)	1.991 (7)	P(1)-C(1)	1.778 (22)
P(1)-C(16)	1.808 (17)	P(1)-C(26)	1.815 (14)
P(2)-S(1)	2.008 (7)	P(2)-C(2)	1.810 (21)
P(2)-C(36)	1.810 (17)	P(2)-C(46)	1.828 (14)
Pb-Au(1)-C(2)	90.1 (5)	Pb-Au(1)-Au(2)′	180.0
C(2)-Au(1)-Au(2)′	89.9 (5)	S(2)-Pb-S(1)′	85.4 (2)
C(2)-Au(1)-C(2)′	179.8 (10)	S(1)-Pb-S(1)′	164.2 (2)
Pb-Au(2)-C(1)	94.3 (5)	Pb-Au(2)-Au(1)′	180.0
C(1)-Au(2)-Au(1)′	85.7 (5)	S(2)-Pb-S(2)′	172.6 (2)
C(1)-Au(2)-C(1)′	171.4 (11)		
Au(1)-Pb-Au(2)	180.0	Au(1)-Pb-S(1)	82.1 (1)
Au(2)-Pb-S(1)	97.9 (1)	Au(1)-Pb-S(2)	93.7 (1)
Au(2)-Pb-S(2)	86.3 (1)	S(1)-Pb-S(2)	95.6 (2)
Pb-S(2)-P(1)	100.9 (3)	Au(2)-C(1)-P(1)	116.3 (11)
Au(1)-C(2)-P(2)	111.9 (11)	P(1)-C(16)-C(11)	121.0 (4)
P(1)-C(16)-C(15)	119.0 (4)	P(1)-C(26)-C(21)	120.5 (5)
P(1)-C(26)-C(25)	119.5 (5)	P(2)-C(36)-C(31)	119.9 (5)
P(2)-C(36)-C(35)	119.9 (5)	P(2)-C(46)-C(41)	118.3 (4)
P(2)-C(46)-C(45)	121.7 (4)	S(2)-P(1)-C(1)	115.7 (7)
S(2)-P(1)-C(16)	107.9 (5)	C(1)-P(1)-C(16)	109.5 (9)
S(2)-P(1)-C(26)	110.3 (5)	C(1)-P(1)-C(26)	108.3 (9)
C(16)-P(1)-C(26)	104.5 (7)	S(1)-P(2)-C(2)	116.1 (6)
S(1)-P(2)-C(36)	111.0 (6)	C(2)-P(2)-C(36)	110.3 (8)
S(1)-P(2)-C(46)	108.1 (5)	C(2)-P(2)-C(46)	105.8 (8)
C(36)-P(2)-C(46)	104.7 (6)	Pb-S(1)-P(2)	100.8 (3)

[a] Estimated standard deviations in the least significant digits are given in parentheses.

(10) (a) Burk, P. J.; Gary, L. A.; Haywood, P. J. C.; Matthews, R. W.; Mcpartlin, M. *J. Organomet. Chem.* **1977**, *136*, C7. (b) Espeas, S.; Husebye, S. *Acta Chem. Scand.* **1974**, *A28*, 309. (c) Jennishe, P.; Olin, A.; Hesse, R. *Acta Chem. Scand.* **1972**, *26*, 15.
(11) Pauling, L. *The Nature of the Chemical Bond*; Cornell Unversity Press: NY, 1967.
(12) Nagle, J. K.; Balch, A. L.; Olmstead, M. M. *J. Am. Chem. Soc.* **1988**, *110*, 319.
(13) Balch, A. L.; Nagle, J. K.; Olmstead, M. M.; Reedy, P. E., Jr. *J. Am. Chem. Soc.* **1987**, *109*, 4123.
(14) Ansell, G. B.; Modrick, M. A.; Bradley, J. S. *Acta Crystallogr.* **1984**, *C40*, 1767.
(15) Blom, N.; Ludi, A.; Burgi, H. B.; Tichy, K. *Acta Crystallogr.* **1984**, *C40*, 1767.

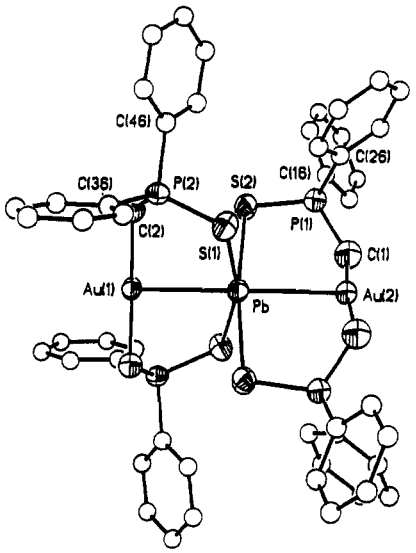

Figure 5. Molecular structure of $Au_2Pb(MTP)_4$ (**3**) showing 50% thermal ellipsoids with the labeling scheme of the atom positions.

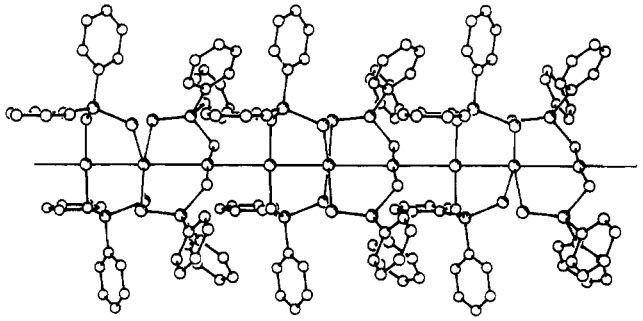

Figure 6. Repeat structure of **3**.

is the first example of a heterobimetallic one-dimensional chain compound containing such short metal–metal (Tl---Au) separations.

The atomic coordinates and thermal parameters for **3** are given in Table IV. Selected bond lengths and distances are listed in Table V. The molecular structure of **3** is shown in Figure 5. The molecule possesses a 2-fold axis on which Au(1), Pb, and Au(2) lie. The Pb atom has an approximate octahedral geometry with two gold atoms on the axial positions and four sulfur atoms on the equatorial postions: S(1)–Pb–S(1)′ = 164.2 (2)°; S(2)–Pb–S(2)′ = 172.6 (2)°. The Pb–S distances, Pb–S(1) = 2.959 (5) Å and Pb–S(2) = 2.976 (6) Å, are quite long but similar to those of $[Pb\{SC(NH_2)_2\}_6]^{2+}$ and $[Pb\{SC(NH_2)_2\}_4]^{2+}$.[16] Again, these bonding interactions are considered to be dominated by ionic forces.

The Au(1)–Pb–Au(2) unit constitutes an extended linear chain along the unique *b* axis, similar to the arrangement found in $Au_2Pt(MTP)_4$ (Figure 6). The Au–Pb distances within the Au–Pb–Au unit are quite different: Au(1)–Pb = 2.896 (1) Å; Au(2)–Pb = 2.963 (2) Å. The sum of metallic radii for Au and Pb is 3.185 Å.[17] Therefore, weak bonding interactions between Au and Pb atoms are likely. The intermolecular distance, Au(1)–Au(2)′ = 3.149 (2) Å, is much shorter than found in $Au_2Pt(MTP)_4$ (3.23 Å) or $Au_2(MTP)_2$ (3.223 (1) Å).[3a] Short intermolecular Au–Au distances have also been found in the sulfur-containing compounds $Au_2(S_2CNBu_2)_2$ (3.02 Å) and $Au_2[S_2P(OR)_2]_2$ (R = *i*-propyl (3.11 Å)).[3]

Compounds with lead–transition-metal bonds are rare. Among the few known bimetallic Pb complexes are $[(PPh_3)_2(Ph)Pt]$-$[Pb(Ph)_3]$[18] (Pt–Pb = 2.698 (8) Å) and $[(\pi\text{-Cp})_2HMo]_2Pb(O_2CMe)_2$[19] (Mo–Pb = 2.808 (1) Å). Complex **3** is the first example showing substantial Au–Pb interactions and also the first example of a one-dimensional polymeric material with the Au–Pb–Au repeat unit.

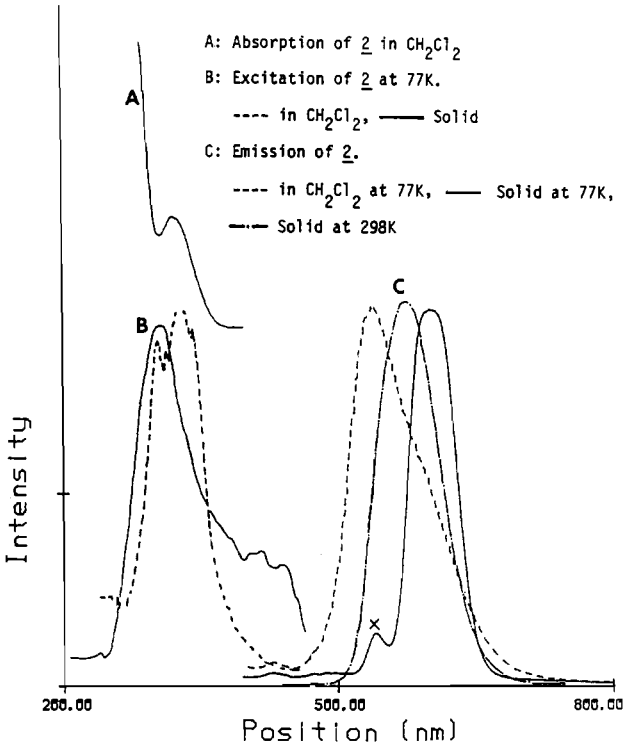

Figure 7. Absorption, excitation, and emission spectra of compound **2**.

Attempts to oxidize **2** and **3** in solution with halogen were unsuccessful. **2** and **3** can be, however, oxidized in the solid. These reactions are currently under investigation in our laboratory.

In compounds **2** and **3** the gold atom has a formal oxidation state of +1 with a $5d^{10}$ configuration, while Tl and Pb atoms have a formal oxidation state of +1 and +2, respectively, with $6s^2$ configurations. No formal metal–metal bonds are expected for these complexes. The bonding interactions of metal atoms in **2** and **3** can be rationalized by understanding the relativistic effects on s orbitals in these heavy-metal atoms, especially the Au atom.[20] These relativistic effects promote the mixing of the empty 6s orbital with the filled $5d_{z^2}$ orbital of the Au atom and the orbitals on Tl and Pb as well. Further evidence for the presence of bonding between metal atoms in these compounds is provided by the interesting low-energy emissions of compounds **2** and **3** and the Fenske–Hall calculations.

Bonding and Properties of Luminescence of $AuTl(MTP)_2$ (2). Excitation, absorption, and emission spectra of the solution and solid of **2** are shown in Figure 7. Crystals of **2** emit an intense yellow-orange color at 575 nm (HW = 2140 cm^{-1}) at 298 K when irradiated with UV light, a higher energy and larger bandwidth than the emission at 77 K (602 nm, HW = 1550 cm^{-1}). Both the emission energy and bandwidth of the solid are temperature-dependent. They decrease with a decrease in temperature. The cause for this interesting observation is not yet understood although it undoubtedly relates to the linear heterobimetallic chain structure of the solid. Emission was not observed for **2** in solution at 298 K, while on freezing of a dilute solution of **2** in CH_2Cl_2 to 77 K, intense yellow emission is observed (536 nm, HW = 3300 cm^{-1}). The excitation spectrum of the frozen solution matches the absorption spectrum of **2** in CH_2Cl_2 at 298 K (maximum 320

(16) (a) Goldberg, I.; Herbstein, F. H. *Acta Crystallogr.* **1972**, *B28*, 400. (b) Herbstein, F. H.; Kaftory, M. *Acta Crystallogr.* **1972**, *B28*, 405.
(17) Sanderson, R. T. *Chemical Periodicity*; Reinhold Publishing Corp.: New York, 1960.
(18) Crociani, B.; Nicolini, M.; Clemente, D. A.; Bandoli, G. *J. Organomet. Chem.* **1973**, *49*, 249.
(19) Kubicki, M. M.; Kergoat, R.; Guerchais, J.-E.; L'Haridon, P. *J. Chem. Soc., Dalton Trans.* **1984**, 1791.
(20) (a) Pyykko, P.; Desclaux, J. P. *Acc. Chem. Res.* **1979**, *12*, 278. (b) Bruce, M. I.; Duffy, D. N. *Aust. J. Chem.* **1986**, *39*, 1697. (c) Jiang, Y.; Alvarez, S.; Hoffmann, R. *Inorg. Chem.* **1985**, *24*, 749. (d) Pitzer, K. *Acc. Chem. Res.* **1979**, *12*, 271.

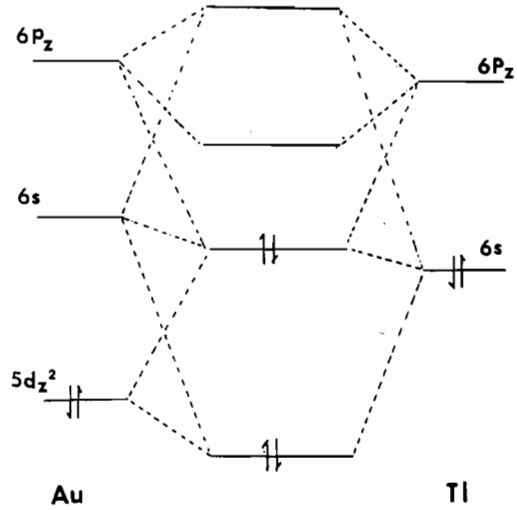

Figure 8. Qualitative molecular orbital diagram for the Au–Tl unit in **2**.

nm, ϵ = 2900 M^{-1} cm^{-1}). A lifetime of 0.98 μs for the decay of the emission from solid **2** at 298 K after laser excitation at 355 nm was obtained. The long lifetime and large separation between excitation and emission peaks indicate that the emission process is phosphorescence.

The emission spectrum of **2** indicates that a Au–Tl interaction is present. PPN[Au(MTP)$_2$] does not absorb at 320 nm, nor does it emit. The Tl(I) ion is luminescent, but its excitation and emission bands are at much higher energies than observed for **2**.[21]

The molecular orbital calculations by Fenske–Hall method[22] indicates that although no formal metal–metal bond is present, there are significant net overlaps of the 6s orbital of Au with the 6p$_z$ orbital of Tl and of the 6p$_z$ orbital of Au with the filled 6s orbital of Tl. This constitutes the major contribution to the σ bonding of the Au–Tl interaction. The HOMO is a σ^* orbital mainly involving the 6s orbital of Tl. The LUMO is a σ orbital that is composed of the 6p$_z$ orbitals of Au and Tl. On the basis of the result of this calculation, a qualitative molecular orbital diagram for Au–Tl bonding in **2** is given in Figure 8. It is proposed that the absorption band at 320 nm, which results in the luminescence of **2**, is from the σ_1^* to σ_2 transition localized on the Au–Tl moiety. The ground-state Au–Tl interaction may be stabilized by the mixing of the filled 6s level on Tl(I) and the filled 5d$_{z^2}$ level on Au(I) with the empty 6s level on Au(I) and a p$_z$ mixing with both levels, a process suggested to be associated with relativistic effects on electrons in these heavy-metal atoms.[20]

Bonding and Properties of Luminescence of $Au_2Pb(MTP)_4$ (3). A THF solution of **3** shows two strong excitation bands at 310 and 385 nm at 298 and 77 K, respectively. These correlate well with the solution absorption spectrum (two maxima: 290 nm, ϵ = 28 598 M^{-1} cm^{-1}; 385 nm, ϵ = 7626 M^{-1} cm^{-1}). A THF solution of **3** shows an intense yellow-green emission at 555 nm (halfwidth = 3070 cm^{-1}) at 298 K with a lifetime of 57 ns, while the frozen solution of **3** shows an intense blue emission at 480 nm (halfwidth = 3400 cm^{-1}) at 77 K with a lifetime of 2.30 μs (Figure 9). The interesting blue shift of the emission band of **3** with the decrease of temperature also has been observed in some other luminescent complexes and is described as "luminescence rigidochromism", i.e. the substantial dependence of the emission maxima on the environmental rigidity.[6] The cause for such phenomena is not fully understood, however.

Very interestingly, solid **3** emits a strong red color at 752 nm (halfwidth = 1240 cm^{-1}) at 298 K with a lifetime of 22 ns. This energy is 4720 cm^{-1} lower than the emission of the solution. This low-energy solid-state emission may be related to the polymeric structure of the compound in the solid state. Attempts to obtain

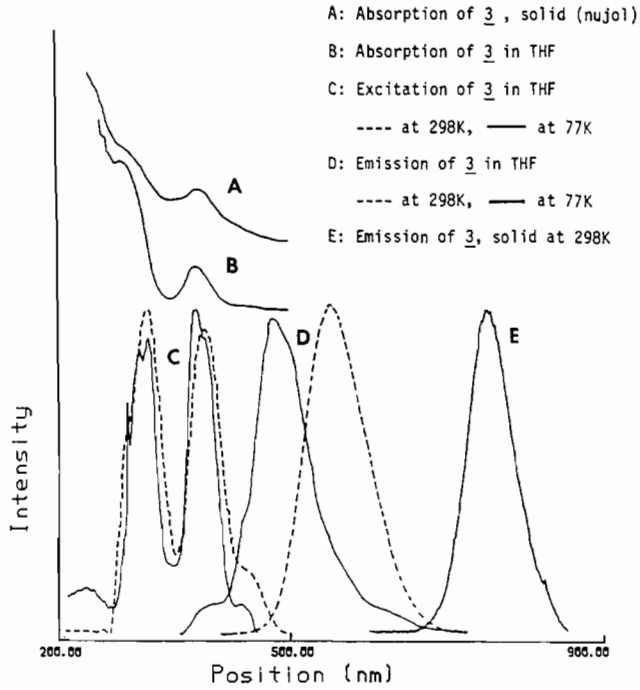

Figure 9. Absorption, excitation, and emission spectra of compound **3**.

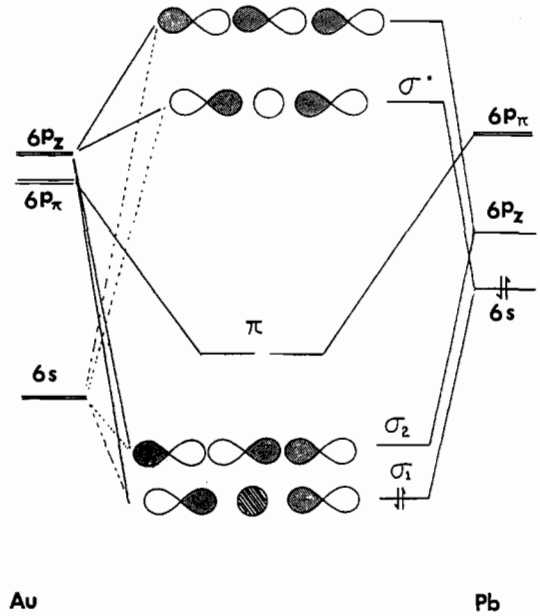

Figure 10. Qualitative molecular orbital diagram for the Au–Pb–Au unit in **3**.

an excitation spectrum of solid **3** failed. However, the absorption spectrum of the solid matches that of the solution in the UV region (Figure 9). A molecular weight measurement for **3** in solution was unsuccessful. ^{1}H NMR spectroscopy and UV–vis absorption and emission spectroscopy over varying concentrations of **3** show no change, suggesting nearly complete formation of monomers.

Sulfur-containing Pb^{II} complexes such as $[Pb(SC(NH_2)_2)_6]^{2+}$ and $[Pb(SC(NH_2)_2)_4]^{2+}$ do not luminesce.[23] The strong solution luminescence of **3** is believed to be a result of Au–Pb–Au interactions. The Fenske–Hall MO calculations show that there are σ-bonding interactions within the Au–Pb–Au unit. They arise mainly from the net overlap of the empty 6p$_z$ orbitals of Au with the filled 6s and the empty 6p$_z$ orbitals of Pb. The empty 6s orbitals of Au are mainly used for the Au–C bonding. However, they also contribute considerably to the M–M σ bonding, as indicated by their net overlap with the 6s and 6p$_z$ orbitals of Pb.

(21) (a) Ranfagni, A.; Mugnai, D.; Bacci, M.; Viliani, G.; Fontana, M. P. *Adv. Phys.* **1983**, *32*, 823. (b) Edgerton, R.; Teegarden, K. *Phys. Rev.* **1963**, *123*, 169.

(22) Hall, M. B.; Fenske, R. F. *Inorg. Chem.* **1972**, *11*, 768.

(23) These compounds were prepared according to literature procedures.[16] They showed no luminescence under UV radiation.

Significant net overlap between the filled 3s and 3p orbitals of the S atoms and the empty $6p_x$ and $6p_z$ orbitals of Pb are believed to be responsible for the weak Pb–S bonds. A qualitative description of the Au–Pb–Au bonding is illustrated in Figure 10. The molecule has approximate S_4 symmetry. The HOMO is a σ-bonding orbital mainly consisting of the $6p_z$ orbital of Au and the 6s orbital of Pb. The LUMO is also a σ-bonding orbital that is nearly entirely constituted from the $6p_z$ orbitals of Au and Pb atoms. The second LUMO is a doubly degenerate π orbital involving the $6p_x$ and $6p_y$ orbitals of Au and Pb atoms, localized mainly on the Au centers. The mixing of the filled $5d_{z^2}$ orbitals of Au with the 6s and $6p_z$ orbitals of Pb is very small and ignored in the MO bonding diagram.

The two absorption bands (or excitation) of **3** in solution probably arise from the two transitions of $\sigma_1 \rightarrow \sigma_2$ and $\sigma_1 \rightarrow \pi$. The transitions from the two excited states to the ground state are probably preceded by a transition to a common relatively stable triplet state through a nonradiative process. The transition from this triplet state to the ground state through the emission of a photon occurs as a phosphorescence. Consequently, only one emission band is observed.

Conclusion

The bimetallic complexes $AuTl(MTP)_2$ and $Au_2Pb(MTP)_4$ are synthesized readily by the reaction of $PPN[Au(MTP)_2]$ with appropriate metal salts. These compounds are the first examples of heterobimetallic one-dimensional chain materials, with repeat units of Au–Tl and Au–Pb–Au. The presence of bonding interactions between metal atoms in these two compounds is supported by the short metal–metal separations in solid state and the strong low-energy luminescence of these compounds in solution and in the solid state. The ground-state metal–metal interaction in these compounds is the result of the mixing of the empty 6s and $6p_z$ orbitals of Au^I with the filled 6s and the empty $6p_z$ orbitals of Tl^I and Pb^{II}.

Experimental Section

General Procedures. All reactions were carried out under N_2 or Ar. Distilled predried solvents were used. $PPN[Au(MTP)_2]$ was prepared as published.[3a,4]

^1H NMR spectra were taken on a Varian XL-200 spectrometer at 200 MHz. ^{31}P NMR spectra were recorded on a Varian XL-200 instrument at 81 MHz. UV–vis spectra were recorded on a Cary Model 17-D spectrophotometer. Emission and excitation spectra were taken on a Spex Fluorolog 2 fluorometer. The excitation source used in emission lifetime measurements at the Center for Fast Kinetic Reactions in Austin was a 10-ns pulse of the 355-nm third-harmonic line of a Quantel YG 481 Nd-YAG laser. The experimental setup is described fully elsewhere.[24] SEM photographs for $Au_2Pb(MTP)_4$ (**3**) were taken in a JEOL JSM-35CF scanning electron microscope without any conductive coating on the sample. SEM photographs for $AuTl(MTP)_2$ (**2**) coated with a Au–Pd alloy (60% Au + 40% Pd, coating thickness = 300 Å) were taken in a JEOL JSM-25S scanning electron microscope. Elemental analyses were done by Desert Analysis Co., Tucson, AZ. Molecular weight measurement was performed at Galbraith Laboratories, Inc., Knoxville, TN. The powder reflectance spectrum was taken on a Perkin-Elmer Lambda 4B UV/VIS spectrophotometer.

Preparation of $AuTl(MTP)_2$ (2). A 40-mg sample of $PPN[Au(MTP)_2]$ (0.038 mmol) was dissolved in 5 mL of CH_2Cl_2. A 10-mg quantity of Tl_2SO_4 (0.020 mmol) in 4 mL of CH_3OH was added to the CH_2Cl_2 solution. The reaction mixture was stirred for 2 h, precipitating a yellow-orange crystalline solid. After filtration, the solid was washed with CH_3OH and diethyl ether a few times and dried in vacuo. Recrystallization of this solid from hot CH_2Cl_2 and diethyl ether yielded 21 mg of pure yellow-orange **2** (0.024 mmol, 64%). Anal. Calcd for $AuTlP_2S_2C_{26}H_{24}$: C, 36.15; H, 2.78. Found: C, 36.65; H, 2.53. ^1H NMR (δ, in $CDCl_3$): 1.62 ppm, d, $-CH_2$, J_{P-H} = 12 Hz; 7.20–7.40 ppm, m, $-C_6H_5$; 7.65–7.80 ppm, m, $-C_6H_5$. ^{31}P NMR (δ, in $CDCl_3$): 50.79 ppm.

Preparation of $Au_2Pb(MTP)_4$ (3). A 45-mg sample of $PPN[Au(MTP)_2]$ (0.043 mmol) was dissolved in 5 mL CH_2Cl_2. A 7-mg quantity of $Pb(NO_3)_2$ (0.021 mmol) in 4 mL of CH_3OH was added to this solution. The solution became yellow immediately. After 10 min of stirring, the solution was cloudy and greenish, and then bronze-colored fiberlike crystals of **3** formed and precipitated from the solution. After 1 h of stirring, the solution was filtered and the solid was washed with CH_3OH and diethyl ether, yielding 23 mg of **3** (0.015 mmol, 72%). **3** can be recrystallized from CH_2Cl_2/ether or THF/ether at 0 °C. When **3** was crystallized from THF/ether solution, two types of crystals were obtained. One is brownish green without THF solvate. The other is red with THF solvate. Both types of crystals have the similar needle shape and interconvert upon THF solvation or desolvation. Anal. Calcd for $Au_2PbP_4S_4C_{52}H_{48}$: C, 40.93; H, 3.15. Found: C, 40.93; H, 3.14. ^1H NMR (δ, in $CDCl_3$): 1.71 ppm, d, $-CH_2$, J_{P-H} = 12 Hz; 7.16–7.38 ppm, m, $-C_6H_5$; 7.65–7.82 ppm, m, $-C_6H_5$. ^{31}P NMR (δ, in $CDCl_3$): 50.55 ppm, $^2J_{Pb-P}$ = 16 Hz.

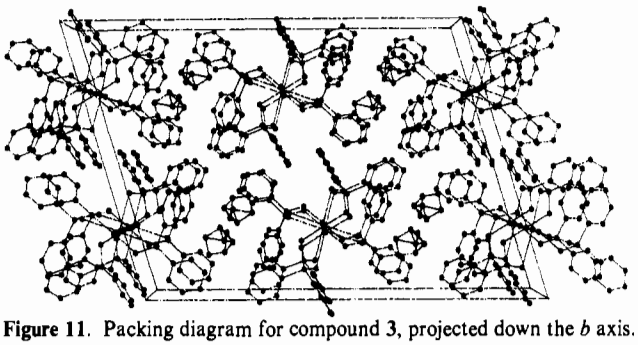

Figure 11. Packing diagram for compound **3**, projected down the *b* axis.

Molecular Orbital Calculations. A detailed description of the approximate Fenske–Hall nonempirical MO method can be found elsewhere.[22] The entire molecule of **2** was calculated by using an atomic basis. The units of $Au(MTP)_2^-$ and $Pb(MTP)_4^{2-}$ in the molecule of **3** were calculated separately at first. The entire molecule of **3** was then calculated by using the same coordinates. The atomic coordinates used in the calculations for **2** and **3** were based on the crystal structure data. The molecules of **2** and **3** were idealized to have C_s and S_4 symmetries to simplify the calculation. For **2**, the averaged bond distances Tl–S = 2.95 Å, Au–C = 2.15 Å, P–S = 2.00 Å, and P–C = 1.88 Å were used. For **3**, the averaged bond distances Au–Pb = 2.93 Å, Au–C = 2.13 Å, Pb–S = 2.97 Å, P–S = 2.00 Å, and P–C = 1.79 Å were used in the calculation. In both cases, the phenyl groups were replaced with H atoms. The local coordinate system for the metal atoms in **2** was chosen such that the *z* axis points toward the center of the Au–Tl vector, the *x* axis is perpendicular to the CAuCTl plane, and the *y* axis is in the plane. The local coordinate system for metal atoms in **3** was chosen as follows: the *z* axes of Au atoms point to the center of the Au–Pb–Au vector, i.e. the Pb atom, the *z* axis of Pb points to one of the Au atoms, and the *x* and *y* axes are in the two AuSPbSAu planes, respectively.

Crystal Structure Determination of 2 and 3 by X-ray Diffraction. Yellow-orange plate crystals of **2** suitable for X-ray diffraction analyses were grown from CH_2Cl_2 solution by slow evaporation of the solvent at 22 °C. Red crystals of **3** with the shape of needles were obtained by slow diffusion of diethyl ether into the THF solution of **3** at 22 °C. The red crystals were solvated with THF. Fast crystallization at 0 °C using mixed solvents of 50% THF/50% diethyl ether yielded brownish green needle crystals without a THF solvate. Unfortunately, these brownish green crystals are not crystallographically suitable single crystals but fibers. Red crystals of **3** containing THF were used for the X-ray diffraction analysis reported here.

Crystals were mounted on glass fibers and sealed with epoxy. Unit cells were determined from 25 machined-centered reflections. Data were collected on a Nicolet R3m/E diffractometer controlled by a Data General Nova 4 minicomputer using Mo Kα radiation at ambient temperature over the range of $2° \leq 2\theta \leq 45°$. Crystals of **2** and **3** belong to the monoclinic crystal system. A body-centered unit cell for **3**, confirmed by systematic absences of $h + k + l = 2n + 1$ in a preliminary data set, was used for the final data collection and structure solution. This choice has the smallest β angle and therefore the least number of correlation problems among the few possible choices of the unit cell.

Standards used for monitoring the crystal of **2** did not show any significant decay, while the crystal of **3** decayed by about 10% during data collection. All data were corrected for decay, absorption, and Lorentz and polarization effects. Empirical absorption corrections were applied for both crystals. Data processing was performed on a Data General Eclipse S140 minicomputer using the SHELXTL crystallographic software (version 5.1).

The space group $P2_1/a$ for **2** was established uniquely from the systematic absences. The space group $I2/a$ for **3** was assumed, and the correctness of this choice was confirmed by the successful solution and refinement of the structure. The positions of metal atoms in **2** were determined by heavy-atom methods. The positions of metal atoms in **3**

(24) Foyt, D. C. *Comput. Chem.* **1981**, *5*, 49.

were determined by direct methods. All non-hydrogen atoms were located by subsequent different Fourier syntheses. Metal, S, and P atoms were refined anisotropically. Phenyl rings were refined as rigid bodies with the fixed C–C distance 1.395 Å and C–C–C angle 120°. The positions of hydrogen atoms on phenyl rings were calculated by using the fixed C–H bond length 0.96 Å. Their contributions were included in the structure factor calculations. The largest peak in the final difference Fourier map of **2**, 3.44 e/Å^3, is 1.82 Å from the Tl atom. The largest peak in the final difference Fourier map of **3**, 0.78 e/Å^3, is 1.39 Å from the Pb atom.

A disordered THF molecule located in the asymmetric unit of **3** was refined successfully. The occupancy factors were refined to 52% for C(4) and C(5) and 48% for C(4)′ and C(5)′, respectively. The packing of **3** with the THF solvate in the lattice is shown in Figure 11. The data used for crystallographic analyses of **2** and **3** are given in Table I.

Acknowledgment. We thank the Welch Foundation, the National Science Foundation (Grant CHE 8708625), and the available fund of Texas A&M University for financial support. We also thank Andy Sargent and Dr. Xue-Jun Feng for their kind help in performing the molecular orbital calculations.

Registry No. **1**, 109638-64-4; **2**, 114057-25-9; **3**·2THF, 123700-53-8; Tl_2SO_4, 7446-18-6; $Pb(NO_3)_2$, 10099-74-8; Au, 7440-57-5; Tl, 7440-28-0; Pb, 7439-92-1.

Supplementary Material Available: Tables of anisotropic thermal parameters and hydrogen atom parameters for **2** and **3** (2 pages); a table of observed and calculated structure factors for **3** (18 pages).

Contribution from the Department of Chemistry, University of Idaho, Moscow, Idaho 83843

Reactions of 5-(Perfluoroalkyl)tetrazolates with Cyanogen, Nitrosyl, and Cyanuric Chlorides

Earnest Obed John, Robert L. Kirchmeier,* and Jean'ne M. Shreeve*

Received May 26, 1989

Sodium tetrazolates, $Na^+\overline{NNNNC}R_f^-$ (R_f = F_2NCF_2 (**4**), C_2F_5 (**5**), CF_3 (**6**)), were formed when sodium azide was added across the triple bond of R_fCN (R_f = F_2NCF_2 (**1**), C_2F_5 (**2**), CF_3 (**3**)). Isomeric mixtures of nitroso, cyano, and cyanuric tetrazolates, $R_f\overline{CNNNN}X$ (R_f = F_2NCF_2, C_2F_5, CF_3; X = NO (**8–10**), CN (**11–13**), $(CN)_3$ (**14–16**)), were obtained by reacting **4**, **5**, and **6** with NOCl, CNCl, and $(CNCl)_3$, respectively. With hydrogen chloride or hydrazoic acid, **4** or **1** gave the stable hygroscopic solid 5-((difluoroamino)difluoromethyl)tetrazoic acid, $NF_2CF_2\overline{CNNNN}H$ (**7**). Stable complexes of tetrazolates **12** and **13**, $[Cu(CF_3\overline{CNNNN}CN)_6][Cu(CF_3\overline{CNNNN})_4]\cdot 2THF$ (**17**) and $[Cu(C_2F_5\overline{CNNNN}CN)_6](C_2F_5\overline{CNNNN})_2\cdot 2THF$ (**18**), were synthesized and characterized by infrared, NMR, and UV spectra, conductivity measurements, and elemental analysis. The ESR study of **17** is also reported.

Introduction

Compounds with high nitrogen content, especially tetrazoles and their salts, are high-energy materials and may explode when exposed to mechanical, thermal, or electrical stimulation.[1-6] Tetrazoles as well as their salts that contain the NF_2 moiety are useful oxidizers when chemically combined with fuels such as anhydrous hydrazine.[7] Sodium azide and hydrazoic acid may undergo 1,3-dipolar[8-16] or HI type addition reactions.[17-27] However, 1,3-dipolar addition is the most commonly observed mechanism in reactions with acetylene and nitriles. An exothermic reaction occurs between sodium azide and (difluoroamino)difluoroacetonitrile,[28] NF_2CF_2CN (**1**), to give sodium 5-((difluoroamino)difluoromethyl)tetrazolate[29] (**4**) in a reaction analogous to that found with R_fCN in which the previously known sodium (perfluoroalkyl)tetrazolates[30] $R_f\overline{CNNNN}^-Na^+$ (R_f = CF_3, C_2F_5) were formed. The enhanced reactivity of perfluoroalkyl nitriles toward tetrazole formation compared to that of nonfluorinated nitriles has been recorded and is not surprising on the basis of the increased electropositive character of the cyano carbon in fluorine-containing nitriles.[31]

Metathetical reactions of sodium 5-(trifluoromethyl)tetrazolate with HCl, Cl_2, and CH_3I gave 5-(trifluoromethyl)tetrazole, 2-chloro-5-(trifluoromethyl)tetrazolate, and an isomeric mixture of 1-methyl-5-(trifluoromethyl)tetrazole and 2-methyl-5-(trifluoromethyl)tetrazole, respectively. Norris[30] isolated individual isomers successfully by fractional distillation. The vibrational

(1) Benson, F. R. *The High Nitrogen Compounds*; Wiley: New York, 1984; Vol. 3, pp 356–366. *Ibid.* Vol. 4, p 394 and references therein.
(2) Morrison, H. *Util. Elem. Pyrotechniques Explos. Syst. Spat., Colloq. Int.* **1968**, 111–120.
(3) Leleu, M. J. *Cah. Notes Doc.* **1978**, No. *92*, 445–449; *Chem. Abstr.* **1979**, *90*, 11461k.
(4) Thiele, J.; Ingle, H. *Justus Liebigs Ann. Chem.* **1895**, *287*, 233.
(5) Silva, J. W.; Staba, E. A. U.S. Patent 3,463,086, 1969.
(6) Staba, E. A. U.S. Patent 3,310,569, 1967.
(7) Kosher, R. J. U.S. Patent 3,394,142, 1968.
(8) Dimroth, O.; Fester, G. *Chem. Ber.* **1910**, *43*, 2219.
(9) Hartzel, L. W.; Benson, F. R. *J. Am. Chem. Soc.* **1954**, *76*, 667.
(10) Mandala, E. O.; Coppola, A. *Att. Accad. Naz. Lincei, Cl. Sci. Fis., Mat. Nat., Rend.* **1910**, *19*, 563; *Chem. Abstr.* **1910**, *4*, 2455.
(11) Huttel, R. *Chem. Ber.* **1941**, *74*, 1680.
(12) Sheehan, J. C.; Robinson, C. A. *J. Am. Chem. Soc.* **1951**, *73*, 1028.
(13) Smith, P. A. S. *Open-Chain Nitrogen Compounds*; Benjamin: New York, 1966; Vol. 2, p 211.
(14) Mandala, E. O.; Noto, F. *Gazz. Chim. Ital.* **1913**, *43* (I), 304. Mandala, E. O. *Gazz. Chim. Ital.* **1914**, *44* (I), 670; **1921**, *51* (II), 195; **1922**, *52* (II), 98; **1915**, *45* (II), 120.
(15) Lieber, E.; Phillai, C. N.; Hites, R. D. *Can. J. Chem.* **1957**, *35*, 832. Lieber, E.; Ramachandran, J. *Can. J. Chem.* **1959**, *37*, 101.
(16) Lieber, E.; Phillai, C. N.; Ramachandra, J.; Hites, R. D. *J. Org. Chem.* **1957**, *22*, 1750. Lieber, E.; Oftedahl, E.; Roa, C. N. *J. Org. Chem.* **1963**, *28*, 194.
(17) Sehaad, R. E. U.S. Patent 2,557,924, 1951.
(18) Knunyants, I. L.; Bykohovskaya, E. G. *Dokl. Akad. Nauk SSSR* **1960**, *131*, 1338; *Chem. Abstr.* **1960**, *54*, 20840.
(19) Banks, R. F.; Moor, G. J. *J. Chem. Soc. C* **1966**, *88*, 2304.
(20) Cleaver, C. S.; Krespan, C. G. *J. Chem. Soc.* **1965**, *87*, 3716.
(21) Andreades, S. *J. Am. Chem. Soc.* **1964**, *86*, 2003.
(22) Boyer, H. J. *J. Am. Chem. Soc.* **1951**, *73*, 5248.
(23) Davies, A. J.; Donald, A. S. R.; Marks, R. E. *J. Chem. Soc. C* **1967**, 2109.
(24) Donald, A. S. R.; Marks, R. E. *Chem. Ind. (London)* **1965**, 1340.
(25) Donald, A. S. R.; Marks, R. E. *J. Chem. Soc. C* **1967**, 1118.
(26) Westland, R. D.; McEwen, W. E. *J. Am. Chem. Soc.* **1952**, *74*, 6141.
(27) Awad, W. I.; Omran, S. M. A. R.; Nagieb, I. *Tetrahedron Lett.* **1956**, *5*, 16.
(28) John, E. O.; Shreeve, J. M. *Inorg. Chem.* **1988**, *27*, 3100. Marsden, H. M.; Shreeve, J. M. *Inorg. Chem.* **1987**, *26*, 169 and references therein.
(29) John, E. O.; Scott, B.; Willett, R. D.; Kirchmeier, R. L.; Shreeve, J. M. *Inorg. Chem.* **1989**, *28*, 893. Emeléus, H. J.; Shreeve, J. M.; Verma, R. D. *Adv. Inorg. Chem.*, in press.
(30) Norris, P. W. *J. Org. Chem.* **1962**, *27*, 3248.
(31) Finnegan, W. G.; Henry, R. A.; Lofquist, R. *J. Am. Chem. Soc.* **1958**, *80*, 3908.

0020-1669/89/1328-4629$01.50/0